AIAA 81-1237R

Shockless Design and Analysis of Transonic Cascade Shapes

Djordje S. Dulikravich*
Universities Space Research Association, Columbia, Maryland
and
Helmut Sobieczky†
DFVLR—Institut für Theoretische Stroemungsmechanik, Goettingen, Federal Republic of Germany

A fast computer program, CAS22, has been developed that can be used in two basic modes: 1) an analysis mode for steady, transonic, potential flow through a given planar cascade of airfoils and 2) a design mode for converting a given cascade into a shockless transonic cascade. The design mode can automatically be followed by the analysis mode, thus confirming that the new flowfield found is shock free. The program generates its own multilevel boundary-conforming computational grids and solves a full-potential equation in a fully conservative form. The shockless design is performed by implementing Sobieczky's fictitious-gas elliptic continuation concept.

Nomenclature

a = speed of sound (isentropic)
a_* = speed of sound (critical)
a_f = speed of sound (fictitious)
c = airfoil chord length
D = determinant: $\partial(x,y)/\partial(X,Y)$
g = y distance between corresponding points on neighboring airfoils
M = Mach number ($M=q/a$)
M_* = critical Mach number ($M_*=q/a_*$)
M_1 = Mach number at upstream infinity
M_2 = Mach number at downstream infinity
n = coordinate direction orthogonal to streamline
P = constant in fictitious-gas relation
q = magnitude of local velocity vector
u,v = components of velocity vector in (x,y) plane
U,V = contravariant components of velocity vector in (X,Y) plane
x,y = Cartesian coordinates in physical plane
X,Y = Cartesian coordinates in computational plane
α_1,α_2 = freestream angles at upstream and downstream infinity
β = cascade stagger angle
γ = ratio of specific heats
θ = angle between x axis and local velocity vector
ν = Prandtl-Meyer function
ρ = isentropic fluid density
ρ_* = critical fluid density
ρ_f = fictitious fluid density
φ = velocity vector potential
ψ = streamfunction

I. Introduction

In the general case of transonic cascade flow, supersonic regions terminate with shocks. These shocks create vorticity and generate entropy in a flowfield that was initially irrotational and homentropic. As a consequence, the aerodynamic drag force sharply increases (wave drag) and the total energy decreases, resulting in a rapid decay of the aerodynamic efficiency of the cascade and an abrupt increase in the aerodynamic noise level. In many experiments it has been observed that, if the Mach number just ahead of the foot of the shock wave is larger than approximately 1.3, the boundary layer starts to separate, leading to complex and potentially dangerous unsteady flow phenomena and mechanical vibrations.

Choked flow represents yet another undesirable phenomenon associated with transonic cascade flow. Choking places an upper limit on the mass flow through a given cascade. As a countermeasure the airfoils in the cascade are often positioned farther apart, decreasing cascade solidity. This results in a decrease in flow turning angle through the cascade and a drop in pressure rise across the cascade.

The main objective of this work is, therefore, to eliminate the shocks (and possibly even the choked flow) by slightly altering certain portions of the contour of a given airfoil in the cascade.

II. Analysis

This work is based on the fictitious-gas concept of Sobieczky[1] and the full-potential, steady, transonic analysis code of Dulikravich.[2] The analysis was derived extensively in earlier works[3,4] and will be repeated here in its concise form only.

In the case of a steady, two-dimensional, irrotational isentropic flow of an inviscid, compressible fluid the conservative form of the continuity equation is

$$(\rho u)_{,x}+(\rho v)_{,y}=0 \tag{1}$$

Equation (1) can also be expressed in its nonconservative, full-potential form

$$\rho\left[\left(1-\frac{\varphi_{,x}^2}{a^2}\right)\varphi_{,xx}-2\frac{\varphi_{,x}\varphi_{,y}}{a^2}\varphi_{,xy}+\left(1-\frac{\varphi_{,y}^2}{a^2}\right)\varphi_{,yy}\right]=0 \tag{2}$$

The canonical operator form[2,5] is

$$\rho(\nabla^2\varphi-M^2\varphi_{,ss})=\rho[(1-M^2)\varphi_{,ss}+\varphi_{,nn}]=0 \tag{3}$$

where (s,n) is the locally streamline-aligned coordinate system.

Equation (3) represents a quasilinear, second-order partial-differential equation of mixed elliptic-hyperbolic type. Equation (1) accepts isentropic discontinuities in its solution.

Presented as Paper 81-1237 at the AIAA 14th Fluid and Plasma Dynamics Conference, Palo Alto, Calif., June 23-25, 1981; submitted July 14, 1981; revision received Jan. 11, 1982.

*Visiting Research Scientist at NASA Lewis Research Center, Fluid Mechanics and Acoustics Division, Computational Fluid Mechanics Branch, Cleveland, Ohio. Presently Assistant Professor in the Department of Aerospace Engineering and Engineering Mechanics, The University of Texas at Austin, Austin, Texas. Member AIAA.

†Section Chief. Member AIAA.

These isentropic shocks satisfy mass conservation

$$M_{a*} M_{b*} = M_{a*}^2 (\rho_a/\rho_b) \tag{4}$$

where M_{a*} and M_{b*} are the values of M_* immediately ahead of and behind the normal shock, respectively. These isentropic shocks differ from the Rankine-Hugoniot shocks formulated as

$$M_{a*} \bar{M}_{b*} = 1$$

Table 1 shows mutual comparison between isentropic and Rankine-Hugoniot shocks calculated for a calorically perfect gas with $\gamma = 1.4$.

Freestream boundary conditions at upstream infinity and at downstream infinity are imposed at the finite cutoff boundaries (Fig. 1). The assumption is that the inflow velocity vector and the outflow velocity vector (the latter obtained iteratively[2] from the global mass conservation) do not vary along their respective boundaries. Periodicity conditions[4] are enforced along the upper and lower boundaries of the flow domain. A constant jump in the potential equal to the circulation is enforced along the cut.

Equation (2) is discretized by using central differencing, except for the points where the flow is locally supersonic. To numerically simulate an analytically proper local domain of dependence of Eq. (2) at supersonic points, a type-dependent,[6] rotated[5] finite differencing is applied to Eq. (3). The result is

$$[\rho(1-M^2)\varphi^H_{,ss} - \rho(1-M^2)\varphi^E_{,ss}] + \rho[\nabla^2\varphi^E - M^2\varphi^E_{,ss}] = 0 \tag{5}$$

Superscript H in Eq. (5) designates upstream differencing, and superscript E designates central differencing to be used for the evaluation of particular second derivatives.

Solution of the steady-state Eq. (3) is obtained by an asymptotic solution to an artificially unsteady[7] equation

$$\rho[(1-M^2)\varphi_{,ss} + \varphi_{,nn} + C_{st}\varphi_{,st} + C_{nt}\varphi_{,nt} + C_t\varphi_{,t}] = 0 \tag{6}$$

for large times, where C_{st}, C_{nt}, and C_t are coefficients. Equation (1) is solved by using an iterative line over-relaxation where consecutive iteration sweeps through the flowfield are considered as steps[4,5] in an artificial time direction. The steady part of the residual (or error) of Eq. (6) is always evaluated by using Eq. (1) supplemented by a directional numerical viscosity in a continuously fully conservative form, thus uniquely capturing possible isentropic shocks. Equation (5) is used for the purpose of constructing a relaxation matrix.[2,9]

For the purpose of a finite difference evaluation of the derivatives in Eq. (5) and a finite area[8] evaluation of the first derivatives in Eq. (1), the flowfield and the governing equations are transformed from the physical (x,y) plane (Fig. 1) into a rectangular (X, Y) computational domain (Fig. 2) by using local isoparametric, bilinear mapping functions.[2,4]

If the geometric transformation matrix is

$$[J]^T = \begin{bmatrix} x_{,X} & y_{,X} \\ x_{,Y} & y_{,Y} \end{bmatrix} \tag{7}$$

then the contravariant velocity components in the (X, Y) plane are

$$\begin{Bmatrix} U \\ V \end{Bmatrix} = [J]^{-1} \begin{Bmatrix} u \\ v \end{Bmatrix} = [J]^{-1}[J^T]^{-1} \begin{Bmatrix} \varphi_{,X} \\ \varphi_{,Y} \end{Bmatrix} \tag{8}$$

Consequently, the fully conservative form of the continuity equation [Eq. (1)] becomes

$$\frac{1}{D}\left((\rho DU)^E_{,X} + (\rho DV)^E_{,Y}\right) + \frac{1}{D}(\xi^H_{,X} + \eta^H_{,Y}) = 0 \tag{9}$$

Table 1 Rankine-Hugoniot ($\bar{M}_{b*}$) and isentropic (M_{b*}, M_b) shock jump relations

M_a	M_{a*}	M_b	$\bar{M}_{b*}$	M_{b*}
1.00601	1.00500	0.99401	0.99500	0.99502
1.01204	1.01000	0.98804	0.99001	0.99010
1.01808	1.01500	0.98210	0.98502	0.98522
1.02415	1.02000	0.97617	0.98003	0.98039
1.03023	1.02500	0.97027	0.97504	0.97561
1.03633	1.03000	0.96439	0.97006	0.97087
1.04245	1.03500	0.95853	0.96508	0.96618
1.04859	1.04000	0.95269	0.96011	0.96154
1.05475	1.04500	0.94687	0.95514	0.95694
1.06093	1.05000	0.94107	0.95017	0.95238
1.06713	1.05500	0.93529	0.94520	0.94787
1.07335	1.06000	0.92952	0.94024	0.94340
1.07959	1.06500	0.92378	0.93528	0.93897
1.08585	1.07000	0.91806	0.93033	0.93458
1.09213	1.07500	0.91236	0.92538	0.93023
1.09843	1.08000	0.90668	0.92043	0.92593
1.10476	1.08500	0.90101	0.91548	0.92166
1.11110	1.09000	0.89537	0.91054	0.91743
1.11747	1.09500	0.88974	0.90560	0.91324
1.12385	1.10000	0.88413	0.90067	0.90909
1.13026	1.10500	0.87854	0.89574	0.90498
1.13670	1.11000	0.87297	0.89081	0.90090
1.14315	1.11500	0.86741	0.88589	0.89686
1.14963	1.12000	0.86188	0.88096	0.89286
1.15613	1.12500	0.85636	0.87605	0.88889
1.16265	1.13000	0.85086	0.87113	0.88496
1.16920	1.13500	0.84538	0.86622	0.88106
1.17577	1.14000	0.83991	0.86132	0.87719
1.18236	1.14500	0.83446	0.85641	0.87336
1.18898	1.15000	0.82903	0.85151	0.86957
1.19563	1.15500	0.82361	0.84662	0.86580
1.20229	1.16000	0.81821	0.84173	0.86207
1.20899	1.16500	0.81283	0.83684	0.85837
1.21571	1.17000	0.80747	0.83195	0.85470
1.22245	1.17500	0.80212	0.82707	0.85106
1.22922	1.18000	0.79678	0.82219	0.84746
1.23602	1.18500	0.79147	0.81732	0.84388
1.24284	1.19000	0.78617	0.81245	0.84034
1.24969	1.19500	0.78088	0.80759	0.83682
1.25656	1.20000	0.77561	0.80272	0.83333
1.26346	1.20500	0.77036	0.79787	0.82988
1.27039	1.21000	0.76512	0.79301	0.82645
1.27735	1.21500	0.75990	0.78816	0.82305
1.28434	1.22000	0.75469	0.78331	0.81967
1.29135	1.22500	0.74950	0.77847	0.81633
1.29840	1.23000	0.74433	0.77363	0.81301
1.30547	1.23500	0.73917	0.76880	0.80972
1.31257	1.24000	0.73402	0.76397	0.80645
1.31970	1.24500	0.72889	0.75914	0.80321
1.32686	1.25000	0.72377	0.75432	0.80000
1.33405	1.25500	0.71867	0.74950	0.79681
1.34128	1.26000	0.71358	0.74469	0.79365
1.34853	1.26500	0.70851	0.73988	0.79051
1.35581	1.27000	0.70345	0.73508	0.78740
1.36313	1.27500	0.69841	0.73028	0.78431
1.37048	1.28000	0.69338	0.72548	0.78125
1.37786	1.28500	0.68837	0.72069	0.77821
1.38527	1.29000	0.68337	0.71591	0.77519
1.39272	1.29500	0.67838	0.71112	0.77220
1.40020	1.30000	0.67341	0.70635	0.76923
1.40771	1.30500	0.66845	0.70157	0.76628
1.41526	1.31000	0.66351	0.69681	0.76336
1.42284	1.31500	0.65858	0.69204	0.76046
1.43046	1.32000	0.65366	0.68728	0.75758
1.43812	1.32500	0.64876	0.68253	0.75472
1.44581	1.33000	0.64387	0.67778	0.75188
1.45353	1.33500	0.63899	0.67304	0.74906
1.46129	1.34000	0.63413	0.66830	0.74627
1.46909	1.34500	0.62928	0.66357	0.74349
1.47693	1.35000	0.62445	0.65884	0.74074

The numerical viscosity[9,10] involving terms

$$\xi = \rho(1-M^2)\frac{D\Delta X}{q^2}(U^2\varphi^E_{,XX} + UV\varphi^E_{,XY})$$

$$\eta = \rho(1-M^2)\frac{D\Delta Y}{q^2}(UV\varphi^E_{,XY} + V^2\varphi^E_{,YY}) \tag{10}$$

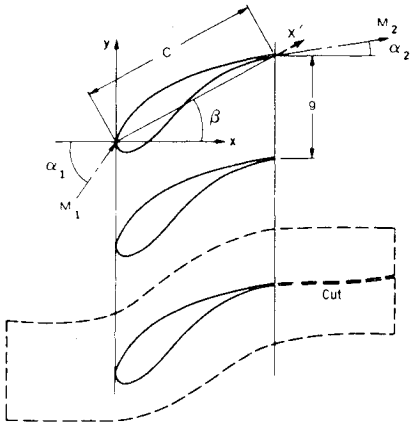

Fig. 1 Planar cascade of airfoils in physical (x,y) plane.

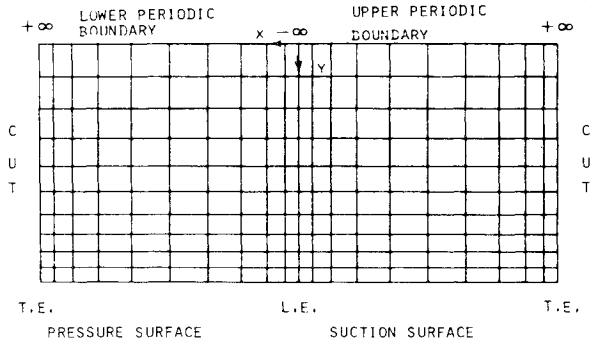

Fig. 2 Periodic flowfield in (X, Y) computational plane.

represents a principal part of the truncation error resulting from the finite difference approximation of the expression

$$[\rho(1-M^2)\varphi^H_{,ss} - \rho(1-M^2)\varphi^E_{,ss}] \tag{11}$$

which appears in Eq. (5).

The computational grid in the (x,y) plane is generated by using a sequence of simple geometric transformations[4] incorporating a single conformal-mapping function, elliptic polar coordinates, and nonorthogonal coordinate stretching and shearing. The uniform grid (Fig. 2) in the computational (X, Y) plane thus remaps back into the periodic, body-fitted, quasiorthogonal grid (Fig. 3) in the physical (x,y) plane. A four-level, consecutive-grid refinement procedure is applied to accelerate the iterative solution of flow equations.

All the flow parameters are nondimensionalized with respect to the critical conditions, denoted by an asterisk, so that the isentropic relations used for the local fluid density and the speed of sound are[11]

$$\frac{\rho}{\rho_*} = \left(\frac{\gamma+1}{2} - \frac{\gamma-1}{2}M^2_*\right)^{1/(\gamma-1)} \tag{12}$$

$$a^2/a^2_* = (\rho/\rho_*)^{\gamma-1} \tag{13}$$

III. Shock-Free Surface Design

Shock-free, or shockless, flow means that the fluid decelerates from a supersonic speed to a subsonic speed not discontinuously (shocked flow) but smoothly over a finite distance (isentropic recompression).

Within the last decade several versions of an indirect (hodograph) shock-free design approach based on Garabedian's method of complex characteristics have been published.[12] The method proved to be a powerful tool for the design of high-performance airfoils and cascades, but handling the complicated boundary- and initial-value problems in a four-dimensional computational space for practically interesting design cases requires considerable experience. It is therefore desirable to develop efficient direct—or nearly direct—design methods.

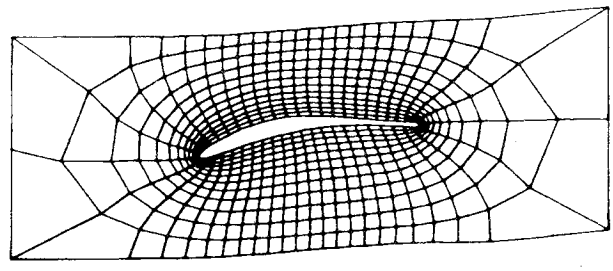

Fig. 3 Computational grid in physical (x,y) plane.

This task was thought to be accomplishable by prescribing a smooth, shock-free pressure distribution along a portion of a given airfoil contour in a cascade and then determining a partially new airfoil shape consistent with the prescribed surface flow conditions. Because of the highly nonlinear character of the transonic flow this design technique generally does not provide an entirely shock-free flowfield.[13] To completely eliminate all shocks (and the associated wave drag) from the flowfield, a number of such designs must be performed, and an optimization technique must be devised to search for a cascade that maintains an entirely shock-free flowfield for a specific set of flow parameters.

IV. Shock-Free Flowfield Design

To eliminate the possibility of obtaining shocks anywhere in the flowfield, Sobieczky proposed[1] and successfully applied[14,15] the concept of a fictitious-gas, shock-free design that corresponds to an elliptic continuation[3] from the subsonic flow domain into local supersonic flow domains. This design technique uses isentropic relations for the fluid density [Eq. (12)] and the speed of sound [Eq. (13)] only where the flow is locally subsonic. At every point where the speed is higher than the local speed of sound, modified (fictitious) relations are used for the fluid density and the speed of sound so that the governing equation remains elliptic throughout the flowfield. Therefore, any conservative computer code capable of solving a subcritical potential flowfield can be modified to include the fictitious-gas concept.

It is important to point out[15] that the flowfield outside the supersonic bubbles calculated from the fictitious-gas relations is already the correct subsonic flowfield. It is only the supersonic parts of the flowfield that still need to be computed and from this recalculation a new portion of the shock-free airfoil surface to be determined. Lift and drag coefficients are also already design results, and they will not be altered by the subsequent recomputation of the local supersonic regions. The sole purpose of originally using a fictitious gas (modified density and speed of sound relation) is thus to determine a shape of the sonic line that is compatible with an entirely shock-free flowfield.

In a two-dimensional planar case of a cascade of airfoils the values of velocity potential φ^* and streamfunction ψ^* on the sonic lines are determined from the fictitious-gas calculation. These values then serve as the initial data for the method of characteristics[1,3] to be used for recomputation of the supersonic zones.[13]

The method of characteristics, now using isentropic gas relations [Eqs. (12) and (13)], is performed inside the triangle ERC of a rheograph[1] plane (Fig. 4). The rheograph plane is defined by the local flow angle θ and the Prandtl-Meyer function $\nu(M_*)$. In this plane the full-potential equation becomes linear[1,3] and the method of characteristics can be

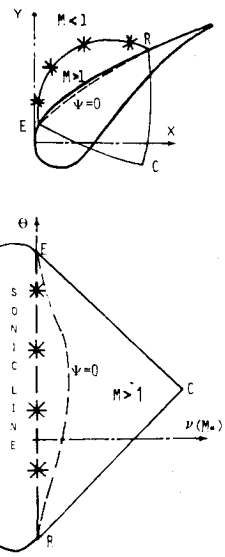

Fig. 4 Physical vs rheograph plane.

applied easily because characteristics become mutually orthogonal straight lines. As a result of this recomputation, the values of φ and ψ are known inside the entire domain ERC, which involves physical and nonphysical parts of the shock-free supersonic zone. The dividing line between these two regions of ERC is a part of the contour of the new shock-free airfoil. The shape of this line is determined from the condition that $\psi = 0$ everywhere on the solid surface. The new shock-free airfoil differs slightly[13] from the original shocked airfoil. The difference exists only in the regions that are wetted by the supersonic flow. The corresponding shock-free supersonic bubble is considerably flatter and somewhat longer than the original shocked[15] supersonic zone.

The fictitious-gas technique is not limited in application to only two-dimensional planar problems such as a hodograph technique; it can be successfully applied to both arbitrary two-dimensional and three-dimensional[14,15] configurations. The airfoil contour closure problem does not exist when applying the fictitious-gas technique.

V. Fictitious-Gas Relations

The fictitious-gas relation ρ_f/ρ_* is applied only in the regions where $M>1$ in order to prevent the governing equation from ever becoming hyperbolic. Nevertheless, any arbitrary analytic expression for ρ_f/ρ_* is subject to several constraints (Fig. 5). It should satisfy the first-order continuity condition on the sonic line of the flowfield; that is,

$$\frac{\mathrm{d}}{\mathrm{d}M_*}\left(\frac{\rho_f}{\rho_*}\right) = -1 \tag{14}$$

when $M=1$. Caughey recently[16] pointed out that, in order to preserve the elliptic character of the full-potential equation, the condition

$$\frac{\mathrm{d}}{\mathrm{d}M_*^2}\left(\frac{\rho_f}{\rho_*}\right) > \frac{-1}{2M_*^2}\left(\frac{\rho_f}{\rho_*}\right) \tag{15}$$

must be satisfied for all values of M_* greater than 1.

It is desirable to use a formula for ρ_f/ρ_* that includes a single (preferably constant) input parameter P that makes the fictitious gas more or less compressible in the supersonic

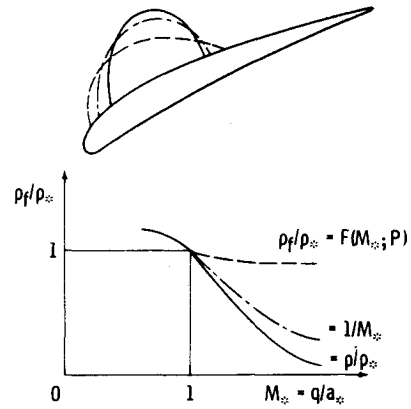

Fig. 5 Sonic line shapes for various density relations.

regions. Such a function must not have minimum or maximum values in the range of expected relative local Mach numbers, because at such points the local fictitious speed of sound a_f/a_* is infinite. This can be observed if the general continuity criterion

$$\frac{\rho_f}{\rho_*} = \exp\left(-\int_{a_*}^{q} \frac{q\mathrm{d}q}{a_f^2}\right) \tag{16}$$

is used to obtain the relation for a_f/a_*. After taking a logarithm and a derivative of both sides of Eq. (16) one gets a general expression for the speed of sound of the fictitious gas

$$\frac{a_f^2}{a_*^2} = -M_* \frac{\rho_f}{\rho_*}\left[1\Big/\frac{\mathrm{d}}{\mathrm{d}M_*}\left(\frac{\rho_f}{\rho_*}\right)\right] \tag{17}$$

For the purpose of guaranteeing an entirely shock-free flowfield the values for ρ_f/ρ_* must always be higher than the values required by the parabolicity condition; that is, $\rho_f/\rho_* = M^{-1}$ (Fig. 5). The final condition for the relation $\rho_f/\rho_* = F(M_*; P)$ is that it should be a very simple function that will also produce a simple expression for a_f/a_*. In the present work we use the relation

$$\frac{\rho_f}{\rho_*} = 1 + \frac{1-\sqrt{1+4P(M_*-1)}}{2P} \tag{18}$$

which gives

$$\frac{a_f^2}{a_*^2} = M_*\left(1 + \frac{1-\sqrt{1+4P(M_*-1)}}{2P}\right)\sqrt{1+4P(M_*-1)} \tag{19}$$

VI. Results

Based on the preceding analysis, computer code[13] CAS22 has been developed and tested for the following sequence of test cases. For the purpose of illustrating basic features of the flow through planar cascades of airfoils the flow around an isolated NACA 0012 airfoil in free air and the flow through a cascade of NACA 0012 airfoils were analyzed. Airfoils in the cascade had zero stagger angle ($\beta = 0$ deg) and a gap-chord ratio of 3.6 ($g/c = 3.6$). The freestream angle was zero at both

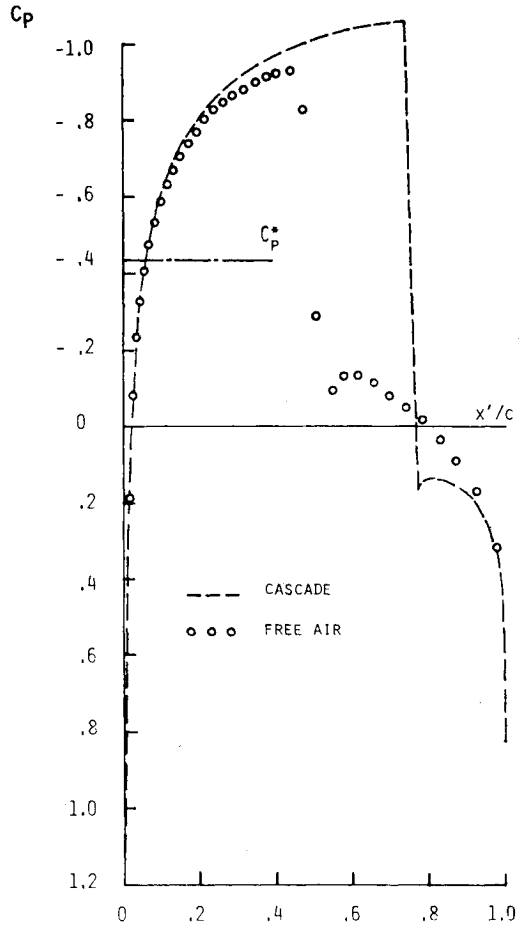

Fig. 6 Transonic cascade effects (airfoil, NACA 0012; $M_1 = M_2 = 0.8$; $g/c = 3.6$; $\alpha_1 = \alpha_2 = \beta = 0$ deg).

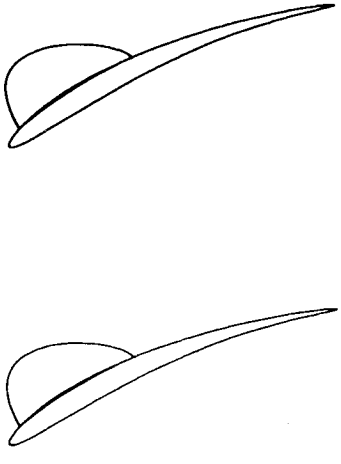

Fig. 7 An original cascade of airfoils with superimposed shock-free redesigned cascade and the corresponding shock-free sonic line shape.

upstream and downstream infinity. In the case of an incompressible freestream ($M_1 = 0.001$) the result obtained for the cascade did not differ from the result obtained for an isolated airfoil.[2] However, in the case of a transonic flow ($M_1 = 0.8$) the cascade effects (Fig. 6) were very significant even for such widely spaced airfoils.

To demonstrate the applicability of shock-free, fictitious-gas design to realistic lifting, staggered cascades, we used a simple analytical shape generator for geometry definition of the input airfoils. Flexible geometry definition is most useful for parametric studies of cascades. Here we used a formula for blade section definition

$$y = Ax + Bx^C + x^{1/2}(1-x)^{1/2}[D + Ex + Fx(1-x)] \qquad (20)$$

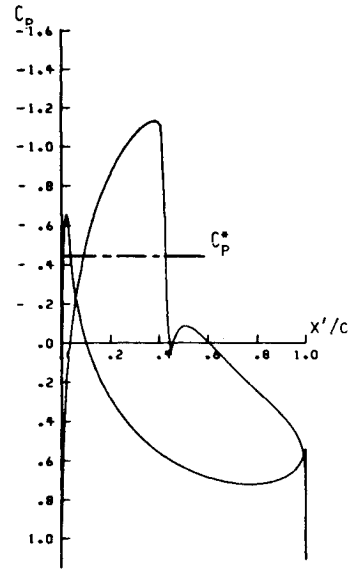

Fig. 8 Analysis of the original cascade ($M_1 = 0.8$; $g/c = 0.85$; $\alpha_1 = 41$ deg; $\alpha_2 = 17$ deg; $\beta = 27.3$ deg).

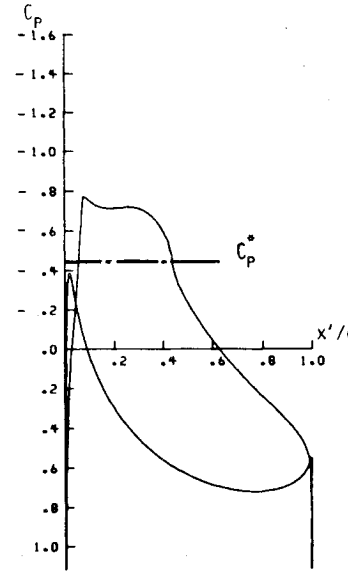

Fig. 9 Shock-free redesign of the original cascade with $P = 25$ in Eqs. (18) and (19).

with a proper choice of the parameters to control leading- and trailing-edge radii, angles, and thickness distribution.

Figure 7 shows two neighboring blades in such a cascade with the superimposed contours obtained from their shock-free redesign. It can be seen that original surface modification is very small and confined to the portion of the suction surface covered by the supersonic flow. The sonic lines shown in Fig. 7 correspond to these new shock-free shapes. The original cascade is strongly shocked (Fig. 8), while its shock-free redesigned version obtained with the design mode of CAS22 code has smooth, shockless recompression (Fig. 9). For this cascade the global flow and geometric parameters were $M_1 = 0.8$, $g/c = 0.85$, $\alpha_1 = 41$ deg, $\alpha_2 = 17$ deg, and $\beta = 27.3$ deg. Then the analysis mode of CAS22 was used to verify that the designed cascade was really shock free (Fig. 10). This step is not necessary, and it served more as a test of the accuracy of the analysis mode of CAS22, which uses first-order artificial viscosity.

This is the first of a series of examples from a parametric cascade airfoil shape study.[17] Although the new cascade loses shock-free properties at off-design conditions (Fig. 11), the resulting shock is still considerably weaker than a shock on the original airfoil. An optimum cascade for a range of operating conditions can be obtained by combining the fic-

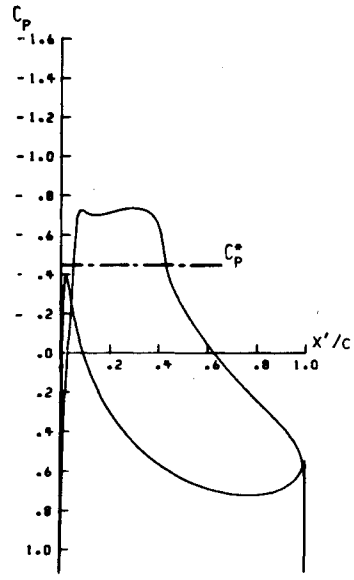

Fig. 10 Analysis verification of the shock-free design.

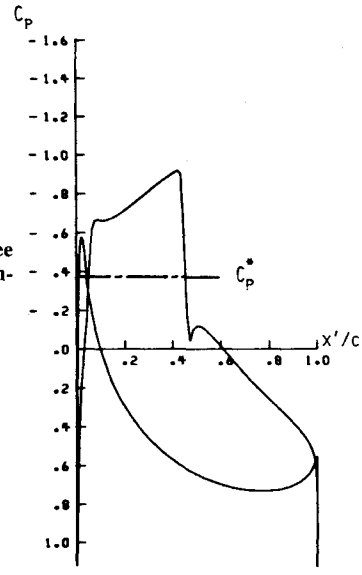

Fig. 11 Analysis of shock-free airfoil at an off-design condition, $M_1 = 0.82$.

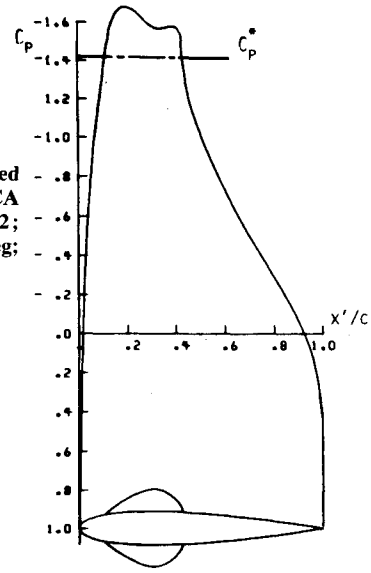

Fig. 12 Unchoking a choked cascade flow (airfoil, NACA 0018; $M_1 = M_2 = 0.582$; $g/c = 1$; $\alpha_1 = \alpha_2 = \beta = 0$ deg; $P = 500$).

titious-gas design concept with an optimization technique.

As already mentioned, computer code CAS22 is capable of converting a choked, shocked cascade flowfield into an unchoked, shock-free flowfield. To illustrate this feature, we selected a nonstaggered cascade of NACA 0018 airfoils with a gap-chord ratio g/c of 1. Note that a simple one-dimensional[11] flow assumption predicts that the flow through this cascade will choke if $M_1 > 0.577$. Therefore, we used the design mode of the CAS22 code with $M_1 = 0.582$ and the fictitious-gas parameter $P = 500$. The resulting flowfield (Fig. 12) was unchoked and entirely shock free.

All the calculations were performed without taking into account viscous boundary-layer effects. For this purpose one may use a standard boundary-layer calculation procedure because shock/boundary-layer interaction effects do not exist in a shock-free flow. The viscous-inviscid calculation can be performed iteratively with a treatment of trailing-edge viscous interaction, as has been demonstrated[18] for isolated supercritical airfoils.

VII. Concluding Remarks

An efficient and reliable computer program, CAS22, has been developed and tested that automatically performs partial redesign of a given airfoil shape in the cascade for the purpose of eliminating shock waves and the associated wave drag. The code represents an application of already known and successfully applied numerical techniques for transonic flow analysis and shock-free flowfield design. These techniques are based on the finite volume and a fictitious-gas approach, respectively. A new formula for the fictitious-gas relation, accompanied with the related physical constraints, has been suggested.

The computer code is entirely self-sufficient in generating its own multilevel boundary-conforming grids. The code can operate separately as a shock-free cascade design code and also as a general transonic cascade analysis program with the capability to accurately capture isentropic shocks.

Acknowledgments

The authors are grateful to their respective research centers for financing this joint research program. Special thanks are due to Mr. Leopold of DFVLR in Goettingen for his help with the computer facilities, to Dr. William McNally of CFM Branch at NASA Lewis for reviewing the manuscript, to Ms. Carol Vidoli for her linguistic expertise and to Ms. Janice Ballinger, Ms. Suzanne Terbrack, and Ms. Florence Sprosty for typing the paper.

References

[1] Sobieczky, H., "Transonic Fluid Dynamics—Lecture Notes," The University of Arizona, TFD 77-01, Oct. 1977.

[2] Dulikravich, D. S., "CAS2D—Fortran Program for Nonrotating Blade-to-Blade, Steady, Potential Transonic Cascade Flows," NASA TP-1705, 1980.

[3] Sobieczky, H., "Rheograph Transformation and Continuation Methods," *Mathematical Methods in Fluid Mechanics,* Von Karman Institute for Fluid Dynamics, VKI-LS-1980-4, Feb. 1980.

[4] Dulikravich, D. S., "Numerical Calculation of Inviscid Transonic Flow Through Rotors and Fans," Ph.D. Thesis, Cornell Univ., 1979; available from Univ. Microfilms, No. 7910741, Ann Arbor, Mich.

[5] Jameson, A., "Transonic Flow Calculations," *Computational Fluid Dynamics,* Vol. 1, Von Karman Institute for Fluid Dynamics, VKI-LS-87-VOL-1, 1976, pp. 1.1-5.84.

[6] Murman, E. M. and Cole, J., "Calculation of Plane Steady Transonic Flows," *AIAA Journal,* Vol. 9, 1971, pp. 114-121.

[7]Garabedian, P., "Estimation of the Relaxation Factor for Mesh Sizes," *Mathematic Tables Aids to Computation,* Vol. 10, 1956, pp. 183-185.

[8]Jameson, A. and Caughey, D., "A Finite Volume Scheme for Transonic Potential Flow Calculations," *Proceedings of AIAA 3rd Computational Fluid Dynamics Conference,* 1977, pp. 35-54.

[9]Dulikravich, D. S. and Caughey, D. A., "Finite Volume Calculation of Transonic Potential Flow Through Rotors and Fans," Cornell Univ., FDA-80-03, 1980.

[10]Dulikravich, D. S., "Numerical Calculation of Transonic Axial Turbomachinery Flows," *7th International Conference on Numerical Methods in Fluid Mechanics,* Stanford Univ., Stanford, Calif., June 1980; also NASA TM-81544, 1980.

[11]"Equations, Tables and Charts for Compressible Flow," NACA TR-1135, 1953.

[12]Garabedian, P. R. and Korn, D. G., "Numerical Design of Transonic Airfoils," *Numerical Solution to Partial Differential Equations, Vol. II—SYNSPADE 1970,* Academic Press, New York, 1978, pp. 253-271.

[13]Dulikravich, D. S. and Sobieczky, H., "CAS22—Fortran Program for Fast Design and Analysis of Shock-Free Airfoil Cascades Using Fictitious-Gas Concept," NASA CR-3507, 1982.

[14]Sobieczky, H., Fung, K-Y., Yu, N., and Seebass, R., "A New Method for Designing Shock-Free Transonic Configurations," *AIAA Journal,* Vol. 17, July 1979, pp. 722-729.

[15]Sobieczky, H., "Design of Advanced Technology Transonic Airfoils and Wings," *Subsonic/Transonic Configuration Aerodynamics, AGARD Fluid Dynamics Panel Symposium,* AGARD CP-285, 1980.

[16]Caughey, D. A., private communications, Oct. 1981.

[17]Sobieczky, H. and Dulikravich, D. S., "Design Examples for Supercritical Cascades," to be published as DFVLR report, 1982.

[18]Nebeck, H. E., Seebass, A. R., and Sobieczky, H., "Inviscid-Viscous Interactions in the Nearly-Direct Design of Shock-Free Supercritical Airfoils," Presented at AGARD FDP Symposium on Computation of Viscous/Inviscid Interaction, 1980.